Characterization of the Fracture Behavior of NBR and FKM Grade Elastomers for Oilfield Applications

Z. Major[1, a] and R.W. Lang[2,b]

[1]Institute of Materials Science and Testing of Plastics, University of Leoben, A

[2]Polymer Competence Center Leoben GmbH, Leoben, A

[a]zoltan.major@mu-leoben.at, [b]reinhold.lang@mu-leoben.at,

Keywords: rapid gas decompression failure, crack initiation and propagation, fracture toughness of rubber, tearing energy, crack tip blunting and opening.

Abstract. In engineering applications elastomers are frequently exposed to complex combinations of mechanical loads (monotonic, static, intermittent and cyclic loads) and additionally might superimposed by various environmental effects. A better understanding of the material resistance against crack initiation and propagation becomes of increasing practical importance, which can be illustrated by the example of the rapid gas decompression failure behavior of pressurized seals for oilfield applications. Modern experimental methods and techniques provide novel opportunities to better understand the deformation and failure behaviour of materials under complex loading conditions. Hence, experiments were performed on both component level under near service loading conditions and on laboratory test specimen level using various specimen configurations for two model elastomers (NBR and FKM). The results are summarized as the kinetics of the loading and the material response. Special emphasis was devoted to the observation and the adequate characterization of the crack initiation and crack growth process by fracture mechanics parameters.

Introduction and Objectives

A phenomenon termed rapid gas decompression (RGD) damage occurs if elastomer seals exposed to high gas pressure fail upon the sudden release of the gas pressure in a brittle manner. The rapid gas decompression failure of elastomer seals is an important issue for the oil exploration industry and recently the objective of an intensive theoretical and practical research [1, 2]

As to the characterization of the rapid gas decompression failure behaviour of pressurized elastomer seals, the paper deals with (i) the instrumented autoclave tests of cylindrical rubber specimens and (ii) the crack initiation and crack growth at high deformation rates and under various constraint conditions. The main objectives of this paper are (i) the characterization of the failure process in elastomers by novel non-contact experimental techniques and (ii) the determination of relevant fracture parameters.

Experimental

Materials Two elastomer types, a HNBR and an FKM type were selected for the investigations described and discussed below. The materials were then produced by the company partner (KF Economos Austria GmbH, Judenburg, A) as O-rings and various test specimens.

Test methods and test set-ups In the first part of the study pressurization/depressurization experiments were performed in an autoclave on specimen level using cylindrical specimens made from two rubber types (HNBR and FKM). The main focus was to develop instrumented experiments, where the pressure and temperature change of the chamber and the expansion of the test specimens were continuously measured and recorded. In the second part of the study fracture

tests were run on a servohydraulic test system (MTS 831.59 Polymer Test System). A single edge notched pure shear specimen configuration with a faint waist in the mid-section (SEN-FWPS specimen) with a nominal thicknesses of 2 mm and unnotched (RBT) and notched cylindrical specimen configuration (CRB specimen) with 14 mm nominal diameter were used in this study. Both single parameter critical tearing energy values and crack growth resistance curves of various elastomer types under monotonic test conditions were determined over a wide loading rate range and the results are analysed based on the crack growth kinetics (da/dt-T curves). The tearing energy values were calculated based on the nominal stress-strain curves of FWPS specimens. For more information on the data reduction please refers to [5].
In addition, to gain more insight into the real material behavior under complex loading conditions full field strain and temperature measurements were performed both in the near crack tip and in the far field in the specimen ligament and subsequently analyzed. Novel test systems like a full-field strain analysis system (Aramis, GOM, Braunschweig, Germany) and an IR-thermography testing system (CEDIP Infrared Systems, France) were used. The Aramis system allows for 2 and 3-dimensional full-field strain analysis whereas the thermo camera can measure temperature distributions across the specimen. Both optical non-contact measuring systems are capable of monitoring tests up to high testing speeds. The complete test system is shown in Figure 1 for RBT test set-up.

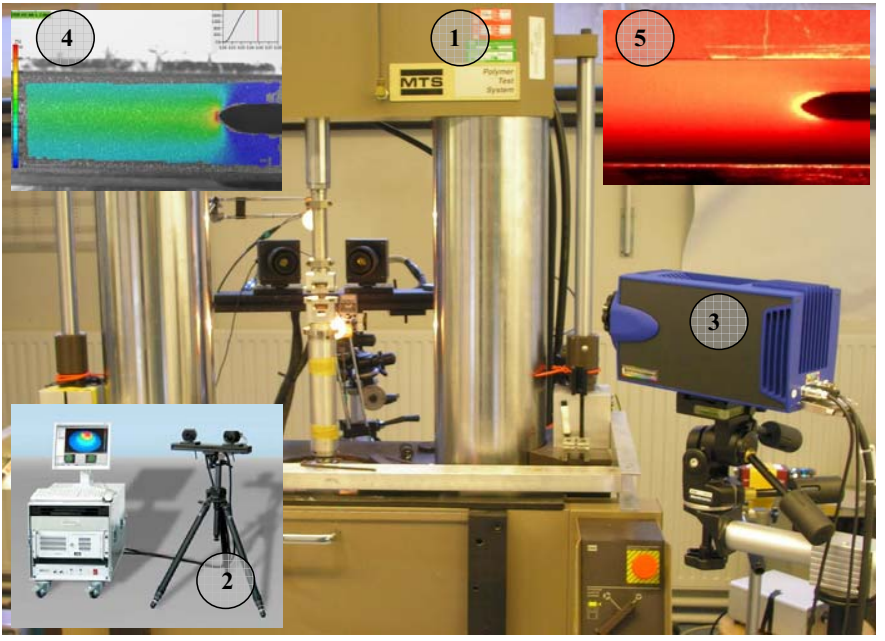

1.. Servohydraulic testing machine, MTS 831.59 Polymer Test System
2.. Aramis full-field strain analysis system
3.. IR-Thermograph camera
4.. Exemplary picture of a FWPS-specimen strain distribution
5.. Exemplary picture of a FWPS-specimen temperature distribution

Fig. 1, Test set-up for the round bar test (RBT) and CRB specimens.

Results and Discussion

The change of the test parameters and the volumetric deformation behaviour of a cylindrical test specimen are shown in Figure 2 during an instrumented RGD test.

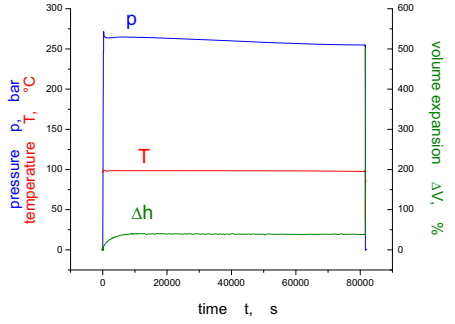

(a)

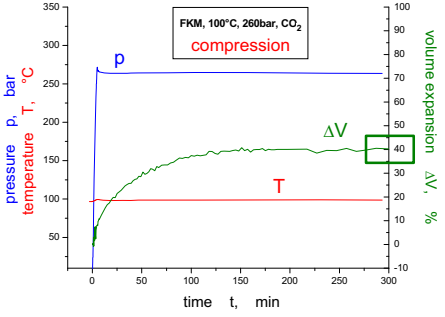

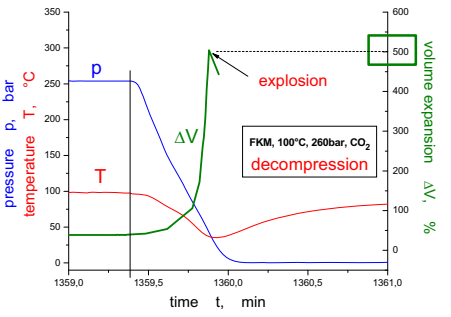

(b) (c)

Fig. 2, The change of the test parameters and the size of the round bar test specimen during an instrumented RGD test; (a) the complete test sequence, (b) pressurization phase and (c) decompression phase.

The various stages of deformation during the pressurization/depressurization phase are also seen in Figure 3. In the pressurization phase a moderate increase of material volume was observed up to the saturation (compare Figures 3a and 3b). After the pressure release a sudden increase of the volume up to very high volumetric strain was observed in a short time (40 % to 500 % in 30 sec, compare Figures 3b and 3c). Finally, an instability of the material and crack appearance on the specimen surface was recognized (see Figures 3d). Based on the diagrams and images depicted above the entire process can be analyzed in detail. Due to the rapid pressure decrease the gas solved in rubber expands and tries to move from the bulk to the free surface of the rubber. During this process a very high degree of volumetric deformation of the elastomer was observed and simultaneously decreasing chamber temperature was recorded. The possible locations of the crack growth initiation are; (i) rubber matrix/filler interface and (ii) the space between particles where the matrix is highly constrained. More detailed analysis of this process can be found in [1-4].

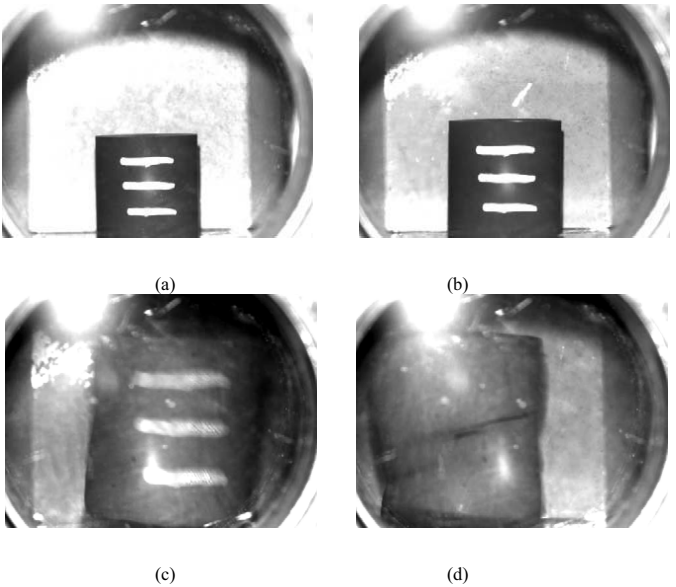

Fig. 3, Volume change of round bar test (RBT) specimen and the appearance of the crack in autoclave; (a) original state, (b) compression phase (saturated), (c) decompression phase (maximal volume strain) and (d) crack appearance.

As the autoclave experiments are very time consuming and expensive, efforts were made to characterize the elastomers by fracture mechanics methods on the laboratory specimen scale. Hence, the correlation between the failure processes in the elastomer grades in the autoclave due to the gas expansion and at the crack tip due to pure mechanical loading was investigated.

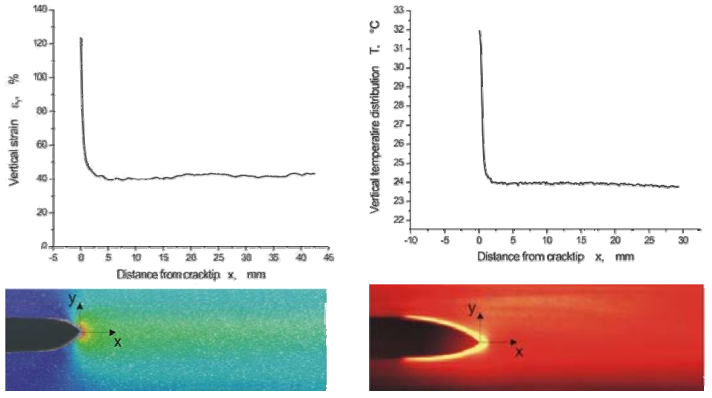

Fig. 5, Strain and temperature distribution of a FWPS specimen at the crack tip and in the ligament; (a) the vertical strain (ε_y) component and (b) the temperature profile is depicted.

Furthermore, the thermo-mechanical effects that take place in the materials during deformation or crack growth respectively were monitored during monotonic tests with unnotched and pre-cracked dumbbell specimens and also using SEN-FWPS specimens. The crack tip temperature of FWPS

specimen is shown at the moment of maximum load in Figure 5 for HNBR. Simultaneously, the strain distribution was also measured and is depicted in Figure 5a. Although, the strain analysis did not work well on the contour edge of the crack, the maximal crack tip strain, ε_{max}^{ct} was estimated. As expected, high strain and temperature gradient was observed in the vicinity of the crack tip. These strain and temperature gradients depend on the crack length on one hand and reveal also pronounced loading rate dependence. In addition to the gradient a higher temperature "crack layer" was also observed.

Load-time-temperature curves of a FWPS specimen at moderate loading rate are seen in Figure 6. The maximum temperature observed at the crack tip region increases simultaneously with the load up to the peak load and than decreases.

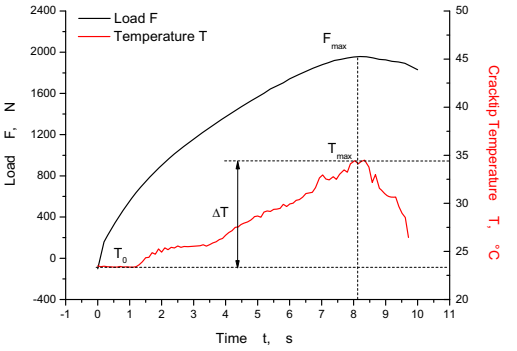

Fig. 6, Load-time-temperature curves of a FWPS specimen for HNBR.

The nominal strain rate dependence of the maximal strain in the vicinity of the crack tip, ε_{max}^{ct} is shown in Figure 7a. A material dependent decrease of the ε_{max}^{ct} values was observed with clear difference between FKM and HNBR. For comparison, based on the global load-displacement curves tearing energy values at the peak load, T_p were calculated and are shown in Figure 7b along with their nominal strain rate dependence. Contrary to the ε_{max}^{ct} values a significant increase of T_p was observed with increasing strain rates.

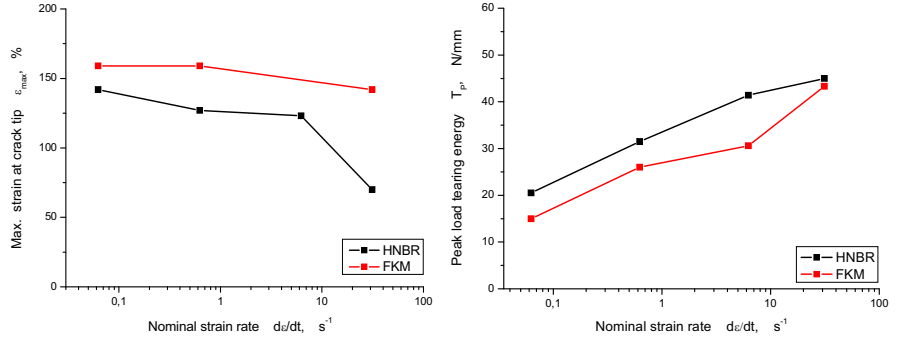

(a) (b)

Fig. 7, Nominal strain rate dependence of (a) the maximal strain at the crack tip, ε_{max}^{ct} and (b) the peak load tearing energy, T_p values for both materials investigated using FWPS specimens.

The kinetics of the crack growth was also analysed and the crack growth rate, da/dt was calculated based on the video sequences. The loading rate dependence of the crack growth rate is shown in Figure 8a for HNBR and in Figure 8b for FKM. While a constant increase of the crack growth rate with increasing crack length with similar slope at all loading rates was observed for HNBR, significant changes are seen in the same curves for FKM. It is assumed that the crack growth is continuous in the FWPS specimen for HNBR and contrary to this, is discontinuous for FKM with crack deceleration and acceleration phases. Latter phenomenon is associated with the crack tip blunting process.

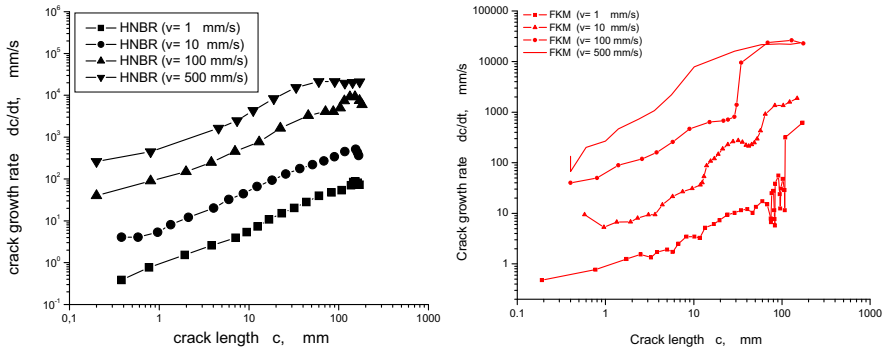

(a) (b)

Fig. 8, Loading rate dependence of crack growth kinetics of; (a) HNBR and (b) FKM.

Hence the crack tip blunting was also analyzed in one specimen during the crack growth. A crack tip opening angle value, CTOA was defined and CTOA values were determined for all specimens. The loading rate dependence of CTOA values is shown in Figure 9a for HNBR and in Figure 9b for FKM. While the CTOA value remains nearly constant during the crack growth process and reveals only small rate dependence for HNBR, significant and with the loading rate increasing changes were observed for FKM (see Figure 10).

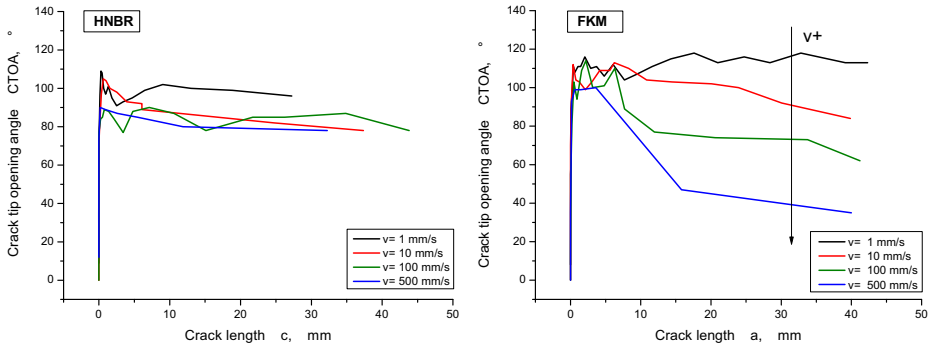

a) (b)

Fig. 9, Loading rate dependence of the crack tip opening angle for; (a) HNBR and (b) FKM.

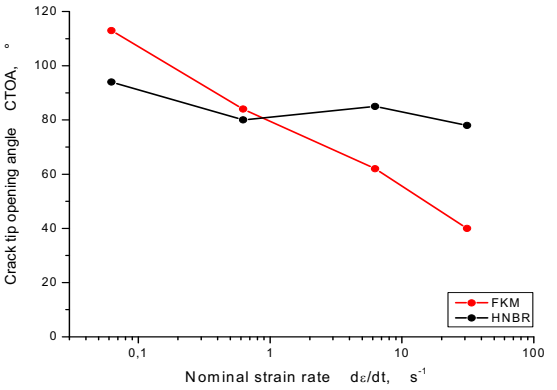

Fig. 10, Nominal strain rate dependence of the crack tip opening angle for materials investigated.

These crack tip deformation processes are schematically summarized in Figure 11. The crack tip blunting is uniform during the entire crack growth process and remains the same over the loading rate range investigated for HNBR elastomer. This results in a continuous crack growth and in a uniform crack growth rate profile. In contrary to this, the degree crack tip blunting changes during the crack growth process. The variation of blunted and sharper crack tip results in continuous and discontinuous crack growth for FKM grade elastomer. The kinetics of this process highly depends on the global (nominal) loading rate of the specimen.

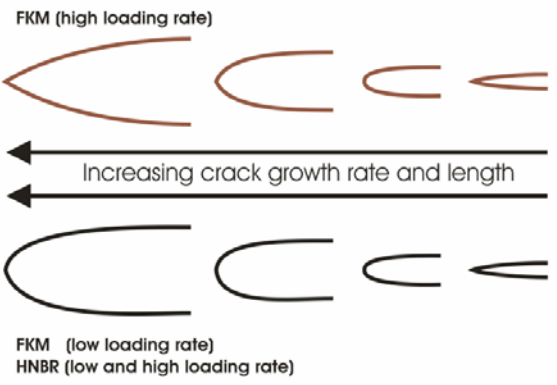

Fig. 11, Schematic presentation of the crack tip deformation process with increasing crack length for both elastomer types investigated.

Summary and Conclusions

To characterize the deformation and failure behavior of elastomers under complex loading conditions, experiments were performed both on component level under near service conditions and

on laboratory test specimen level using two model elastomer grades selected. To gain more insight into the material response novel non-contact full-field strain and temperature analysis methods and techniques were applied. The kinetics of the loading process and the material response was measured, recorded and analyzed in terms of directly measured quantities (pressure, temperature, force, strain). Moreover, based on these measurements global and local fracture mechanics parameters were also calculated and the materials were compared.

The findings of these experiments are summarized below:
The crack initiation and crack growth in RGD process occurs due to the high volume deformation and are favored by the highly multiaxial stress state both on a macroscopic and on a microscopic scale. High material temperatures were measured in the specimens during the fracture process and with increasing loading rate increasing maximum temperatures were observed. On the other hand a decreasing temperature was measured in the pressure chamber during the decompression. It is assumed that the resultant of these two opposite tendencies is a highly non-uniform temperature profile in the bulk material during the RGD process. Material grade and loading rate dependent distinct crack tip blunting was observed in the test specimens. A uniform blunting process goes hand in hand with a continuous crack growth and in contrary with a non-uniform blunting process a discontinuous crack growth was observed. While an increase of global peak tearing energy, T_p values with increasing loading rate was observed, the local deformation based fracture parameters, maximal crack tip strain, ε_{max}^{ct} and the crack tip opening angle, CTOA was found to clearly decrease with increasing loading rates for both materials. As overall conclusion it is stated that simple fracture experiments on laboratory specimen scale does not sufficiently reflect the very complex loading situation in RGD and can not yield adequate material parameters. However, these experiments provide useful information both about the fracture behavior as well as input data for further modeling and simulation work.

Acknowledgement

The research work for this paper was performed at the Polymer Competence Center Leoben GmbH (PCCL, A) within the framework of the K_{plus}-programs of the Austrian Ministry of Traffic, Innovation and Technology with the contributions of the University of Leoben as scientific partner and the Economos Austria as company partner. The PCCL is founded be the Austrian Government and the State Governments of Styria and Upper Austria.

References

[1] B.J. Briscoe, T. Savvas and C.T. Kelly, Explosive decompression failure of rubber, Rubber Chemistry and Technology, Vol. 67, 384-416, 1994

[2] C.J. Derham and B. Thompson, Mechanisms of explosive (rapid gas) decompression and related phenomena in elastomers (rubbers) and thermoplastics, 4th Oilfield Engineering with Polymers, MERL, 3-4 November, London, 2003, 7-28.

[3] Z. Major et al., Development of a test and failure analysis methodology for elastomeric seals exposed to explosive decompression, 5th Oilfield Engineering with Polymers, MERL, 29-30 March, London, 2006, Paper 10.

[4] B. Flaconnèche. M.H. Klopfer and C. Taravel Condat, 5th Oilfield Engineering with Polymers, MERL, 29-30 March, London, 2006, Paper 7.

[5] C. Feichter, Z. Major and R.W. Lang, Fatigue crack growth in elastomers - Part I: Theoretical background, test procedure and data reduction, submitted to RC&T, 2007.